coordinate. The resultant parameters were fitted to a cubic spline function of RC[3,21] and are provided as supplementary material.

The potential of mean force (pmf) for the Menshutkin reaction in water was obtained through Monte Carlo statistical perturbation calculations.[11] Precise evaluation of the free energy difference at different values of RC was achieved using $\Delta G(RC_1) - \Delta G(RC_0) = -RT \ln \langle \exp(-[H(RC_1) - H(RC_0)]/kT) \rangle_{H(0)}$, where $\langle\ \rangle_{H(0)}$ represents an ensemble average corresponding to the Hamiltonian $H(RC_0)$, while $H(RC_1)$ is the Hamiltonian for the perturbed system. The simulation was carried out by moving the RC forward and backward at intervals of ±0.1 Å when |RC| ≤ 1.0 Å and of ±0.15 Å for other regions. Thus, a total of 30 simulations was executed to cover the whole reaction. All calculations were performed for the reactants plus 750 water molecules in a rectangular box at 25 °C and 1 atm using the NPT ensemble. As in previous studies, periodic boundary and preferential sampling techniques were employed to enhance the solute–solvent statistics.[18] An equilibration period of 1×10^6 configurations was followed by 1.5×10^6 configurations for averaging for each run. The standard deviations ($\pm\sigma$) were computed from fluctuations of separate averages for blocks of 1×10^5 configurations. All computations were performed on a SUN SPARCstation 2 and a STARDENT 3030 computer in our laboratory; the Monte Carlo simulations required ca. 15 days.

In Figure 1, the computed free energy profile, or pmf, for the Menshutkin reaction of $H_3N + CH_3Cl$ in water was compared with that in the gas phase. The solution-phase curve was anchored to the computed total free energy of hydration of the reactant molecules.[20] Therefore, Figure 1 represents an absolute free energy scale. Clearly, solvation leads to a tremendous stabilization of the products and a large decrease of barrier height. The most striking finding in the present study is that there is a shift of 0.4 Å on the transition state toward the reactants, in accord with empirical expectations.[9,10] It should be noted, however, that the observed TS shift is entirely due to the solvent effects since solute geometries were kept fixed during the Monte Carlo simulations. Inclusion of internal degrees of freedom may result in additional changes of the TS in solution. The charge separation at the TS was ca. 70% as predicted from Mulliken population analysis using various basis sets, which is consistent with previous estimates.[22] The computed free energy of reaction in water, −37 ± 2 kcal/mol from the pmf or −32 ± 2 kcal/mol from the hydration free energies,[20] may be compared with the experimental data (−34 ± 10 kcal/mol).[23] This represents a decrease of ca. 155 kcal/mol due to solvation. The agreement emphasizes the validity of the potential functions used in the present study and supports the computational procedure.

The computed activation free energy of 25.6 ± 1 kcal/mol is a reduction of 21 kcal/mol relative to the gas-phase process. Experimental data do not appear to be available for this particular reaction; however, comparison can be made to an activation *energy* of 23.5 kcal/mol for the reaction of $H_3N + CH_3I$ in water.[24] Interestingly, a unimodal reaction profile in water was also obtained for the Menshutkin reaction, a result similar to that found in the previous chloride exchange reaction.[2a,25] Further analysis of the present Menshutkin reaction in water will be presented later.[26]

Supplementary Material Available: Details of the potential function and geometrical parameters along with the Fortran subroutines for the cubic spline fitting (8 pages). Ordering information is given on any current masthead page.

(26) Gratitude is expressed to the donors of the Petroleum Research Fund, administered by the American Chemical Society, for partial support. Computational assistance from Prof. J. D. Madura and Xinfu Xia is gratefully acknowledged.

Structure of Dilithiobenzenide: An ab Initio Study

Andrzej Sygula* and Peter W. Rabideau*

Department of Chemistry, Louisiana State University Baton Rouge, Louisiana 70803

Received April 23, 1991

In a recent communication, Sakurai et al.[1] reported a determination of the crystal structure of bis[(tetrahydrofuran)lithium(I)] hexakis(trimethylsilyl)benzenide (**1**). They found the six-membered ring to be significantly folded, forming a boat, with the lithium cations located on the same side of the ring (syn-facial) in surprisingly short distance from one other (2.722 Å). Because of the serious steric hindrance expected in **1**, a question arises as to whether the crystal structure data may serve as an appropriate

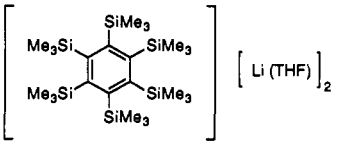

1

model for dilithiobenzenide itself. The latter compound is of great theoretical interest, although not observed experimentally. Herein we report the results of the first ab initio calculations on monomeric, unsolvated dilithiobenzenide that resolve the above question.

Preliminary MNDO[2] calculations provided two minima, **2** and **3**: one with syn- and the other with an anti-facial arrangement of the lithium cations. MNDO predicts **3** to be more stable by

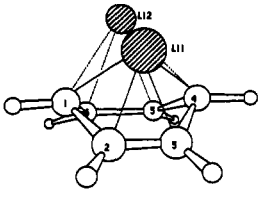

2 (C_{2v})

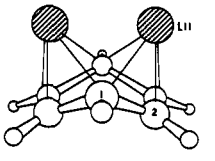

2 (rear view)

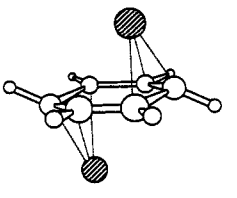

3 (C_{2h})

6.6 kcal/mol. Ab initio[3] optimization of the MNDO structures

(21) (a) Gerald, C. *Applied Numerical Analysis*; Addison-Wesley: Reading, MA, 1980; pp 474–488. (b) Press, W. H.; Flannery, B. P.; Teukolsky, S. A.; Vetterling, W. T. *Numerical Recipes*; Cambridge University Press: New York, 1989; pp 86–89.

(22) (a) Abraham, M. H. *Prog. Phys. Org. Chem.* **1974**, *11*, 1. (b) Abraham, M. H. *J. Chem. Soc. B* **1971**, 299; *Chem. Commun.* **1970**, 293.

(23) The experimental free energy of reaction was computed from a thermodynamic cycle using experimental free energies of hydration and gas-phase reaction free energy. See refs 16 and 20.

(24) (a) Okamoto, K.; Fukui, S.; Shingu, H. *Bull. Chem. Soc. Jpn.* **1967**, *40*, 1920. (b) Okamoto, K.; Fukui, S.; Nitta, I.; Shingu, H. *Bull. Chem. Soc. Jpn.* **1967**, *40*, 2354.

(25) A 180° flipping of the methylammonium cation results in a more stable ion pair with Cl^- in the gas phase; however, the free energy difference was only 0.6 ± 0.2 kcal/mol in water in favor of the rotamer at RC = 1.5 Å. This indicates that, unlike in the gas phase, conformation swapping after bond breaking is insignificant in aqueous solution.

(1) Sekiguchi, A.; Ebata, K.; Kabuto, C.; Sakurai, H. *J. Am. Chem. Soc.* **1991**, *113*, 1464.

(2) Dewar, M. J. S.; Thiel, W. *J. Am. Chem. Soc.* **1977**, *99*, 4899. Lithium parameters taken from MNDOC: Thiel, W. *QCPE* **1982**, *2*, 63. The MNDO calculations were performed without symmetry restrictions, but led to C_{2v}(**2**) and C_{2h}(**3**) local minima.

0002-7863/91/1513-7797$02.50/0

Table I. Calculated Total Energies (au), Relative Energies (kcal/mol), and Zero-Point Energies (kcal/mol) for the Haptomers of Dilithiobenzenide

compd	3-21G//3-21G [ZPE[a]]	6-31G*//6-31G* [ZPE[a]]	MP2/ 6-311G*//6-31G*
2 (C_{2v})	−244.179 406 (0.0)[b] [68.7]	−245.543 876 (0.0)[b] [68.5]	−246.449 312 (0.0)[b]
5 (C_1)	−244.157 816 (13.5)[b] [67.1]	−245.525 933 (11.3)[b] [67.0]	−246.430 334 (11.9)[b]

[a] Uncorrected. [b] Relative energy.

at the HF/3-21G level with the above defined symmetry restrictions led to two stationary points (Table I). Theoretical vibrational analysis proved **2** to be a true minimum, but **3** turned out to be a transition state (one negative vibration, 212*i*; E(RHF) = −244.142 253 au, 23.3 kcal/mol above **2**). Following the transition vector, we located another stationary point **4**, with C_s symmetry (E(RHF) = −244.157 011 au, 14.1 kcal/mol above **2**) that again appeared to be a transition state with one imaginary frequency (182*i*). Finally structure **5** with C_1 symmetry and no

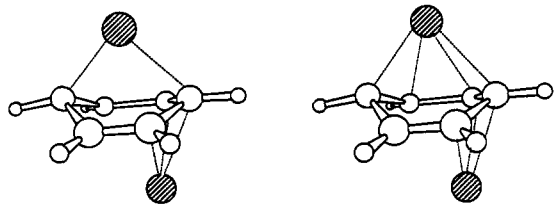

4 (C_s) 5 (C_1)

negative frequencies was found to be a true potential energy minimum for the anti-facial haptomer of dilithiobenzenide. Geometries of **2** and **5** were then reoptimized at the HF/6-31G* level and again characterized by theoretical vibrational analysis showing them to be true minima at this level of theory as well. The 6-31G* optimal geometries for **2** and **5** were used for single-point calculations at the MP2/6-311G* level (Table I). The syn-facial haptomer **2** is more stable than the anti-facial analogue **5** at all levels of approximation employed. At the MP2/6-311G*//6-31G* level with zero-point energy (ZPE) correction, the energy difference is 10.4 kcal/mol in favor of **2**. It may be concluded that **2**, which is quite similar to the structure found in the crystal state for the hexakis(trimethylsilyl) derivative **1**, is a global minimum of monomeric, unsolvated dilithiobenzenide.

It should be noted, however, that the calculated total energy of **2** is still higher than the energy of the potential substrates, benzene and two lithium atoms. The formal reaction

$$C_6H_6 + 2Li \rightarrow \mathbf{2}$$

is endothermic by +13.4 kcal/mol at the 6-31G*//6-31G* level—the exact number may be slightly higher due to basis set superposition error. Nonetheless, this is consistent with the experimental difficulties associated with the preparation of unsubstituted dilithiobenzenide.[4]

Comparison of bond lengths and angles calculated with both 3-21G and 6-31G* basis sets with the X-ray structure determination data[1] for **1** (Table II) reveals some interesting features. First of all the differences between the calculated and experimental values are small considering that the calculated values are for isolated dilithiobenzenide while the crystal structure of **1** includes solvation by two THF molecules and substitution with six TMS groups. The experimental bond lengths are generally slightly longer than the calculated ones, and this is easily understood in terms of both substitution and solvation effects. The main features of the dilithiobenzenide system in both the calculated and experimental structures are very similar. For example, the C(1)–C(2) distance is much longer than C(2)–C(3), and the Li–C(2) bond is significantly shorter than Li–C(1). Also, the bond angle C(2)–C(1)–C(6) is lower than C(1)–C(2)–C(3) in both calculated **2** and experimental **1**. Moreover, the surprisingly short Li–Li distance in **2**[1] is also predicted by the calculations (see Table II).

Table II. Comparison of Selected Bond Lengths and Angles Calculated for **2** with the Experimental Values of **1**

bond length (Å) or angle (deg)[a]	3-21G	6-31G*	exptl[b]
C(1)–C(2)	1.4935	1.4818	1.493–1.526
C(2)–C(3)	1.3532	1.3527	1.386–1.400
Li(1)–C(1)	2.2677	2.2855	2.296–2.496
Li(1)–C(2)	2.0824	2.0735	2.099–2.127
Li(1)–Li(2)	2.4102	2.4306	2.722
C(1)–H(1)	1.0765	1.0786	
C(2)–H(2)	1.0748	1.0784	
C(2)–C(1)–C(6)	108.9	109.6	107.4–108.6
C(1)–C(2)–C(3)	115.7	116.1	113.3–116.1
folding angle	129.1	131.0	126.0

[a] See structure **2**. Li(1) is over C(1)–C(2)–C(3)–C(4), and Li(2) is over C(1)–C(6)–C(5)–C(4). [b] Reference 1.

Perhaps the most interesting result is that the calculated folding angle of the benzene ring in **2** (129.1 or 131.0° at the 3-21G and 6-31G* level, respectively) is very close to the value of 126° found in the crystal state for **1**.[1] This angle is significantly smaller (that is, the degree of folding is higher) than the angle calculated at the 6-21G level for the benzene dianion in the singlet state (167°).[5] Although this difference was previously attributed to steric factors in **1**,[1] our results show that significant folding of the benzene ring in dilithiobenzenides, as compared to the benzene dianion, results from interactions of the lithium cations with the benzene dianion moiety. Apparently the steric repulsions of the TMS groups in **1** do not lead to serious structural deformations in the dilithio derivative as they do in the parent hexakis(trimethylsilyl)benzene.[6]

In conclusion, calculations suggest that the syn-facial haptomer of monomeric, unsolvated dilithiobenzenide **2** is more stable than the anti-facial analogue **5**. This is in contrast with the ion triplet concept[7] as well as with both theoretical[8] and experimental[9] results available for benzannelated analogues such as dilithionaphthalenide and dilithioanthracenide in which the anti-facial arrangement of the lithium cations is favored.[10] Moreover, the calculated lowest energy structure **2** resembles closely the crystal structure of bis[(tetrahydrofuran)lithium] hexakis(trimethyl-

(3) GAUSSIAN 88: Frisch, M. J.; Head-Gordon, M.; Schlegel, H. B.; Raghavachari, K.; Binkley, J. S.; Gonzalez, C.; Defrees, D. J.; Fox, D. J.; Whiteside, R. A.; Seeger, R.; Melius, C. F.; Baker, J.; Martin, R. L.; Kahn, L. R.; Stewart, J. J. P.; Fluder, E. M.; Topiol, S.; Pople, J. A. Gaussian, Inc., Pittsburgh, PA.

(4) (a) See for example: Buncel, E. In *Comprehensive Carbanion Chemistry*; Buncel, E., Durst, T., Eds.; Elsevier: New York, NY, **1980**, Chapter 1. (b) Stevenson, G. R.; Zigler, S. S.; Reiter, R. C. *J. Am. Chem. Soc.* **1981**, *103*, 6057. (c) Deposition of lithium with benzene on argon matrix is believed to produce (among others) $Li_2C_6H_6$ complex, but its structure has not been investigated: Manceron, L.; Andrews, L. *J. Am. Chem. Soc.* **1988**, *110*, 3840.

(5) Podlogar, B. L.; Glauser, W. A.; Rodriguez, W. A.; Raber, D. J. *J. Org. Chem.* **1988**, *53*, 2129.

(6) Sakurai, H.; Ebata, K.; Kabuto, C.; Sekiguchi, A. *J. Am. Chem. Soc.* **1990**, *112*, 1799.

(7) Streitwieser, A., Jr. *Acc. Chem. Res.* **1984**, *17*, 353.

(8) Sygula, A.; Lipkowitz, K.; Rabideau, P. W. *J. Am. Chem. Soc.* **1987**, *109*, 6602.

(9) (a) Brooks, J. J.; Rhine, W. E.; Stucky, G. D. *J. Am. Chem. Soc.* **1972**, *94*, 7346. (b) Rhine, W. E.; Stucky, G. D. *J. Am. Chem. Soc.* **1975**, *97*, 2079.

(10) Although in both dilithionaphthalenide and dilithioanthracenide the lithium cations are not associated with the same benzene ring in the lowest energy haptomers,[8,9] they still show the general features of the ion triplet—the lithiums are located on the opposite sides of the negative charge cloud of the organic dianion.

silyl)benzenide showing the latter to be an appropriate model for the experimentally unobserved dilithiobenzenide.

Acknowledgment. This work was supported by the Division of Chemical Sciences, Office of Basic Energy Sciences of the U.S. Department of Energy, and SNCC (Louisiana State University) for allocation of computer time.

Self-Assembly of Porphyrins on Nucleic Acids and Polypeptides

Robert F. Pasternack* and Antonino Giannetto

Department of Chemistry, Swarthmore College Swarthmore, Pennsylvania 19081

Pamela Pagano and Esther J. Gibbs*

Department of Chemistry, Goucher College Towson, Maryland 21204

Received May 28, 1991

The free-base porphyrin *trans*-bis(*N*-methylpyridinium-4-yl)-diphenylporphine (*trans*-H_2P_{agg}) organizes under appropriate conditions of concentration and ionic strength, into extended assemblies on single-stranded (ss) and double-stranded (ds) DNA templates.[1,2] The ability to arrange porphyrins into helical domains provides opportunities for the construction of supramolecular-based chemical devices having, for example, useful conduction, magnetic, and catalytic properties. Such applications will require assemblies of metalloderivatives, and in the present report, we consider the effect of metalation on solution and nucleic acid binding properties of this cationic porphyrin. We also present evidence that, in addition to nucleic acid templates, polypeptides can serve to organize these species.

Supramolecular porphyrin structures of the type considered here give rise to unprecedentedly large induced circular dichroism signals in the Soret region.[1,2] We suggested that (1) these signals arise from long-range coupling of transition dipole moments of the porphyrin molecules as they orient on the helical backbone of DNA and (2) this organization is a manifestation of the tendency of *trans*-H_2P_{agg} to aggregate. We consider here the solution properties of *trans*-$Cu^{II}P_{agg}$ and *trans*-$Au^{III}P_{agg}$[3] and report on the CD signals obtained on the binding of these metal derivatives to DNA.

Addition of sodium chloride to an aqueous solution (no DNA added) of *trans*-CuP_{agg} leads to marked spectral changes. There is a large bathochromic shift of the Soret band from 417 to 440 nm with significant hypochromicity and deviation from Beer's law behavior. In these respects, the copper(II) derivative behaves very much like the free-base *trans*-H_2P_{agg} porphyrin (and a number of anionic porphyrins which are known to aggregate in solution[4,5]). In contrast, addition of salt up to 0.2 M has little influence on the spectrum of *trans*-AuP_{agg} and Beer's law is obeyed by this chromophore at the Soret maximum of 401 nm. From these results we conclude that whereas the copper derivative of *trans*-H_2P_{agg} aggregates (as does the nonmetallo form), the gold(III) derivative does not.

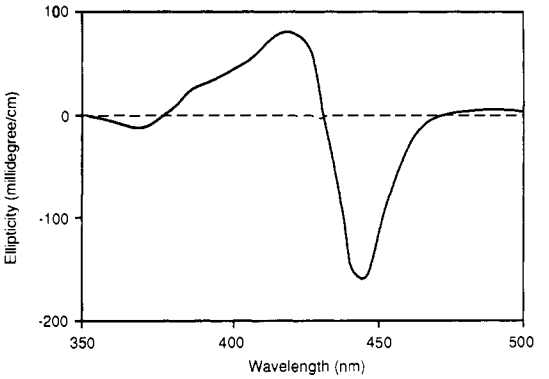

Figure 1. Induced circular dichroism spectra for the *trans*-CuP_{agg}/DNA complex at two different ionic strengths; [*trans*-CuP_{agg}] = 5 μM, [DNA] = 40 μM. At [NaCl] = 0.010 M, a single negative feature is obtained (---) having a magnitude of about 2 mdeg. The signal obtained at [NaCl] = 0.17 M (—) is vastly different in profile and magnitude.

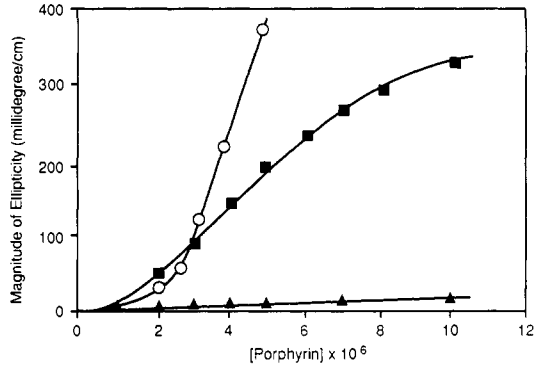

Figure 2. Induced circular dichroism spectra for several porphyrin/DNA complexes as a function of porphyrin concentration: (■) *trans*-H_2P_{agg} at [DNA] = 40 μM, [NaCl] = 0.10 M, λ = 449 nm (negative portion of profile); (○) *trans*-CuP_{agg} at [DNA] = 70 μM, [NaCl] = 0.17 M, λ = 425 nm (positive part of profile); (▲) *trans*-AuP_{agg} at [DNA] = 40 μM, [NaCl] = 0.10 M, λ = 414 nm (at single, negative feature). The concentration dependences of the induced CD signal, S, for the aggregating derivatives can be fit by an equation of the form $S = a[\text{porph}]^n/(1 + b[\text{porph}]^n)$ where $a = 1.33 \times 10^{13}$, $b = 3.05 \times 10^{10}$, and $n = 2$ for *trans*-H_2P_{agg}; $a = 4.15 \times 10^{18}$, $b = 2.93 \times 10^{15}$, and $n = 3$ for *trans*-CuP_{agg}. In contrast, the plot for *trans*-AuP_{agg} is linear, $S = 1.15 \times 10^6[\text{porph}]$.

Under conditions of low ionic strength, where there is little tendency for charged meso-substituted porphyrins to aggregate,[1,4,5] both metal derivatives, like the parent *trans*-H_2P_{agg}, produce only a single, small negative CD feature in the Soret region *when bound to calf thymus (ct) DNA*. From our previous work with a variety of porphyrins, we have determined that this induced negative CD band is characteristic of an intercalated porphyrin molecular ion.[6] This result parallels those obtained for the Cu(II) and Au(III) derivatives of tetrakis(*N*-methylpyridinium-4-yl)porphine (CuT4 and AuT4).[3,6] However, unlike the results obtained with the nonaggregating CuT4 and AuT4 derivatives, adding salt to the *trans*-H_2P_{agg}/DNA or *trans*-CuP_{agg}/DNA complex leads to dramatic changes in the absorption (about a 15-nm bathochromic shift with some hypochromicity) and CD spectra in the Soret region (see Figure 1). The dependence on porphyrin concentration of the magnitude of the CD signals of *trans*-CuP_{agg}/DNA and *trans*-H_2P_{agg}/DNA is shown in Figure 2. (It is important to note that there is no evidence from CD signals of the DNA polymer light scattering experiments for DNA condensation under these conditions.[1,7]) The nonaggregating *trans*-AuP_{agg} derivative, on the other hand, behaves differently from the *trans*-H_2P_{agg} and *trans*-CuP_{agg} species and instead provides CD signals with DNA much like those of AuT4; i.e., throughout the salt and metallo-

(1) Gibbs, E. J.; Tinoco, I., Jr.; Maestre, M.; Ellinas, P. A.; Pasternack, R. F. *Biochem. Biophys. Res. Commun.* **1988**, *157*, 350.

(2) Pasternack, R. F.; Brigandi, R. A.; Abrams, M. J.; Williams, A. P.; Gibbs, E. J. *Inorg. Chem.* **1990**, *29*, 4483.

(3) The metalloderivatives were prepared via minor modification of literature methods. See: Bütje, K.; Nakamoto, K. *Inorg. Chim. Acta* **1990**, *167*, 97. Gibbs, E. J.; Maurer, M. C.; Zhang, J. H.; Reiff, W. M.; Hill, D. T.; Malicka-Blaszkiewicz, M.; McKinnie, R. E.; Liu, H. Q.; Pasternack, R. F. *J. Inorg. Biochem.* **1988**, *32*, 39. The Soret maximum of *trans*-CuP_{agg} in aqueous solution (no salt added) is at 417 nm ($\epsilon = 2.34 \times 10^5$ M^{-1} cm^{-1}) while that of *trans*-AuP_{agg} is at 401 nm ($\epsilon = 2.23 \times 10^5$ M^{-1} cm^{-1}).

(4) Pasternack, R. F.; Huber, R. P.; Boyd, P.; Engasser, G.; Francesconi, L.; Gibbs, E.; Fasella, P.; Venturo, G. C.; Hinds, L. C. *J. Am. Chem. Soc.* **1972**, *94*, 4511.

(5) Pasternack, R. F.; Francesconi, L.; Raff, D.; Spiro, E. *Inorg. Chem.* **1973**, *12*, 2606.

(6) Pasternack, R. F.; Gibbs, E. J.; Villafranca, J. J. *Biochemistry* **1983**, *22*, 2406.

(7) Phillips, C. L.; Mickols, W.; Maestre, M. F.; Tinoco, I., Jr. *Biochemistry* **1986**, *25*, 7803.

0002-7863/91/1513-7799$02.50/0